



ELECTRICAL PROPERTIES OF MULTILAYER ULTRATHIN PERMALLOY /CR/ PERMALLOY THIN FILMS

¹*Mustafa Erkovan, ²Mustafa Okutan, ¹Sait Eren San and ¹Osman Ozturk¹Department of Physics, Gebze Institute of Technology, Gebze, 41400, Kocaeli, Turkey²Department of Physics, Yildiz Technical University, Davutpasa, 34210 Istanbul, Turkey

ARTICLE INFO

Article History:

Received 25th December, 2012

Received in revised form

29th January, 2013Accepted 24th February, 2013Published online 19th March, 2013

Key words:

A: Alloys,

A: Thin films,

B: Magnetron Sputtering

D: Electrical conductivity,

D: Dielectric properties.

ABSTRACT

Multilayer ultrathin films of Cr/Ni₈₀Fe₂₀/Cr/Ni₈₀Fe₂₀/Cr were grown on p-type Si substrate by magnetron sputtering deposition. Thickness dependencies of multilayer thin films were analyzed with impedance spectroscopy. The samples were characterized in a frequency range of 100k – 40M Hz under different DC bias voltages varying from 0 to 1 V. The dependence of relaxation time on the dielectric relaxation frequency was determined from the Cole-Cole plots for different thicknesses two ultrathin permalloy /Cr/ permalloy thin films. The values inferred from Cole-Cole plots suggest that this is a Debye-type dielectric relaxation process under DC bias and we propose that this result is due to the dipolar structure of the samples and the capacitive nature of the interfaces between adjacent layers.

Copy right, IJCR, 2013, Academic Journals. All rights reserved.

INTRODUCTION

Multilayered metallic thin films are of critical importance in material science (Heinrich *et al.*, 1991). The magnetic properties of these films have been extensively investigated due to their technological applications (Binasch *et al.*, 1988; Baibich *et al.*, 1988). Unlike their magnetic properties, the dielectric properties of the multilayered thin films (MTFs) have not been well studied, although these films are promising elements in electronic applications. There has been very little work on the impedance spectroscopy (IS) of MTFs (Galán, Calzada and Pardo 2004). Different growth methods of thin films were also studied by impedance spectroscopy technique (Kek-Merl, Lappalainen and Tuller 2006). MTFs are fabricated by the consecutive deposition of alternating layers of materials, such as Co, Fe, Ni and permollays, and they are separated by a nonmagnetic layer. Noble metals like Ag, Au, and Cu are commonly used as the nonmagnetic layer. Some additional nonmagnetic materials such as Cr, Pt, Pd and Ru have also been studied (Wigen and Zhang 1992). In this paper, we explored the impedance properties of two MTF samples with different ultrathin layer thicknesses. The order of the layers in these samples were Si/Cr 50 Å/Ni₈₀Fe₂₀ 30 Å / Cr X / Ni₈₀Fe₂₀ 30 Å/ Cr 100 Å where X = 15 and 20 Å. A small variation of the Cr layer thickness and the outer oxide Cr layer substantially alters the electrical properties of the whole system.

Experimental

Sample Preparation

The multilayer films were prepared by magnetron sputtering deposition. Sputtering is a widely used deposition technique in thin film fabrication which allows the fast deposition of both insulators and metals. It allows the facile control of deposition parameters during the process. Moreover, this technique is readily used in industry for the fabrication of magnetic materials, facilitating the

technology transfer required for the large scale production of novel materials with interesting applications (du Tremolet de Lacheisserie, Gignoux and Schlenker 2005). Actually this assembly was investigated from magnetic point of view in (Topkaya *et al.*, 2010) and in the scope of our work, effect of the layer was evaluated from the point of view of electrical properties. We have prepared two MTF samples on p-type Si (100) substrate including spacers made up of Cr layers with different thicknesses. Metallic targets had three inches diameter. Ni₈₀Fe₂₀ layers were deposited at rate of 0.07 Å/sec using a radio frequency (RF) magnetron gun operating at 20 Watt power. A direct current (DC) magnetron gun operating at 30 Watt power was employed for the Cr layer deposition. The deposition rate for this layer was 0.4 Å/sec. The deposition rates of Cr and Ni₈₀Fe₂₀ were determined by X-Ray photoelectron spectroscopy (XPS). The base and deposition pressures were 3×10⁻⁹ mbar and 1.6×10⁻³ mbar, respectively. Argon (99.9999 %) was used as the sputtering gas. Circular Ag electrodes with 1 mm radius and 1000 Å thickness were deposited by thermal evaporation after the fabrication of the MTFs. Schematic representation of the MTF samples are depicted in Figure 1.

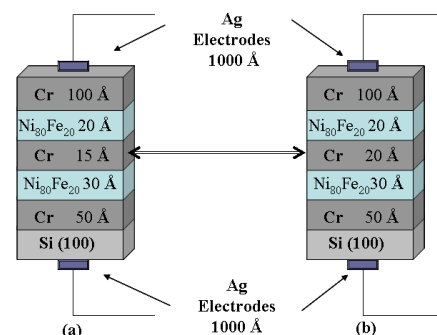


Figure 1. Schematic representation of MTFs with layer Cr thickness of a) 15 Å, b) 20 Å.

Electrical Measurements

AC dielectric properties were analyzed from the dielectric values measured at different DC bias voltages. A HP 4194A impedance analyzer was utilized in these measurements. Complex dielectric response was measured in a frequency range of 100k to 40M Hz. RMS amplitude was set to ~ 495 mV. The data was recorded at room temperature.

RESULTS AND DISCUSSION

The complex dielectric constant ϵ is expressed in terms of the real ϵ' and imaginary ϵ'' components, which represents the stored and dissipated energy components of the material, respectively. The dielectric constant is expressed as

$$\epsilon(\omega) = \epsilon'(\omega) + i\epsilon''(\omega) \quad (1)$$

The real part of the dielectric constant ϵ' of a material is the normalized permittivity with respect to the permittivity of vacuum. It is also a measure of the amount of polarization in a material according to (Knight and Nur 1986) and can be indirectly calculated from the following equation using the capacitance data,

$$\epsilon' = C_p d / (\epsilon_0 A), \quad (2)$$

where C_p is the parallel capacitance, d is the inter electrode distance, ϵ_0 is the permittivity of the free space and A is the sample area. The energy loss ϵ'' is given by

$$\epsilon'' = \epsilon' \tan \delta \quad (3)$$

where $\delta = 90 - \varphi$ and φ is the phase angle. Tangent loss ($\tan \delta$) is also a typical dielectric parameter. Figure 2ab shows for bias 0 voltages the real and the imaginary parts of the dielectric constant of the MTFs as a function of frequency for two different thicknesses of Cr layer. The dielectric constant values increased with the increasing Cr thickness for most parts of the frequency range, but the effect was more pronounced at higher frequencies. Frequency dependent Cole-Cole form of Equation 1 is expressed as (Raju 2003),

$$\epsilon^* = \epsilon_\infty + \frac{(\epsilon_0 - \epsilon_\infty)}{1 + (i\omega\tau)^{1-\alpha}} \quad (0 \leq \alpha \leq 1) \quad (4)$$

where ϵ_0 and ϵ_∞ are the low and the high frequency dielectric values, respectively, in the measured frequency interval, ω is the angular frequency, τ is the relaxation time, and α is the absorption coefficient.

The frequency dependent real part of the dielectric constant can be derived using Eq.1 and 4 as (Raju 2003) [10]

$$\epsilon'(\omega) = \epsilon_\infty + (\epsilon_0 - \epsilon_\infty) \cdot \frac{1 + (\omega\tau)^{1-\alpha} \sin \frac{1}{2} \alpha\pi}{1 + 2(\omega\tau)^{1-\alpha} \sin \frac{1}{2} \alpha\pi + (\omega\tau)^{2(1-\alpha)}} \quad (5)$$

This equation implies that the real part of the dielectric constant is expected to decrease if the dielectric medium in the sample is subject to an electric field. ϵ_∞ value approaches zero at higher frequencies while ϵ_0 can take various values at low frequencies at different voltages. The curves in Figure 2ab are fitted to Equation 5 whereby the relaxation times (τ) and the absorption coefficients (α) were

acquired. Table 1 depicts the fitting results from 0V bias in Figure 2a. Both τ and α values decreased with the increasing Cr layer thickness. ϵ' values start to change only below a certain relaxation dielectric frequency, which can be determined via plots of ϵ'' as shown in Figure 2cd. The relaxation dielectric frequency (f_c) decreases substantially with the increasing Cr layer thickness. It is a general trend that the real part of the dielectric constant decreases with the increasing frequency in such films. The dielectric strength ($\Delta\epsilon$) parameter is given in reference (Şentürk 2004) as,

$$\Delta\epsilon = \epsilon_0 - \epsilon_\infty \quad (6)$$

It is also observed that the dielectric strength $\Delta\epsilon$ decreases with the increasing Cr layer thickness. We have also analyzed the effect of Cr layer thickness under DC bias and examined the Debye behavior of these films by equivalent circuit analysis. The frequency dependence of the real and the imaginary parts of the dielectric constant were measured at various DC bias voltages (Figure 2). Dielectric strength ($\Delta\epsilon$) values were calculated from the ϵ' plots. $\Delta\epsilon$ values at five different DC bias voltages are given in Table 2. Electronic circuit behaviors were determined in terms of DC and AC voltage dependencies in a certain frequency range. Imaginary parts of the dielectric constants of MTFs are also plotted in Figure 2. As depicted in Figure 2c, maximum values of ϵ'' did not change with the application of DC bias and the dielectric relaxation frequency (f_c) increases with the increasing DC bias for the 15 Å thick Cr layer sample. However, for the sample with 20 Å thick Cr layer, maximum values of ϵ'' decreases with the increasing DC bias although the dielectric relaxation frequency (f_c) further increases as depicted in Figure 2d. The maximum point in the semi-logarithmic plots of the imaginary dielectric constant gives the dielectric relaxation frequency (f_c) values which are presented in Table 2. The dependence of the relaxation time τ on the DC bias can be calculated by using (Park *et al.*, 2005),

$$\tau = 1 / (2\pi f_c) \quad (7)$$

The calculated τ values from the fits of plots are in agreement with the critical frequency based calculations from Figure 2. Table 2 shows these critical frequency based results. The existence of Debye type relaxation can be determined from the Cole-Cole plots. As shown in the insets of Figure 3, the centers of the arcs are located below the x-axis for both samples, indicating that non-Debye type relaxation is dominant when there is no applied bias. The non-Debye type relaxation implies that the conductivity exhibits a non-exponential relaxation in time domain (Macedo, Moynihan and Bose 1972). As the DC bias is increased, the centers of the arcs move above the x-axis, suggesting that the relaxation process becomes Debye type. In regard to the equivalent circuit; the interfacial capacitance C_1 due to the interface between the Si substrate and the metallic multilayer is considered to be in series with the R_1 resistance of the layers. The applied DC bias reinforces a C_2 component parallel to the $R_1 C_1$ circuit. In the Cole-Cole plots, a second circle does not form and the growth is linear after the first arc. This indicates that a second resistive component with R_s is connected in series to the rest of the circuit. The equivalent circuit diagram for a MTF structure is depicted in Figure 4. The applied DC bias reduces the effect of the series resistance (R_s) and results in the switching from non-Debye to Debye type relaxation. ϵ_{max} values were also determined from the Cole-Cole plots (Figure 3). ϵ_{max} values tend to decrease with the increasing DC bias as shown in Table 2. Frequency dependence of the relaxation time τ decreases as the Cr layer thickness increases and τ exponentially decreases with the increasing DC bias. These two important trends are explicitly demonstrated in Figure 5. A small increase of 5 Å in the Cr layer thickness nearly doubles the relaxation

time when there is no applied bias. This suggests that the increasing Cr layer thickness reduces the restoring force. However, the difference in the relaxation times declined with the increasing applied bias which acted as an additional restoring component.

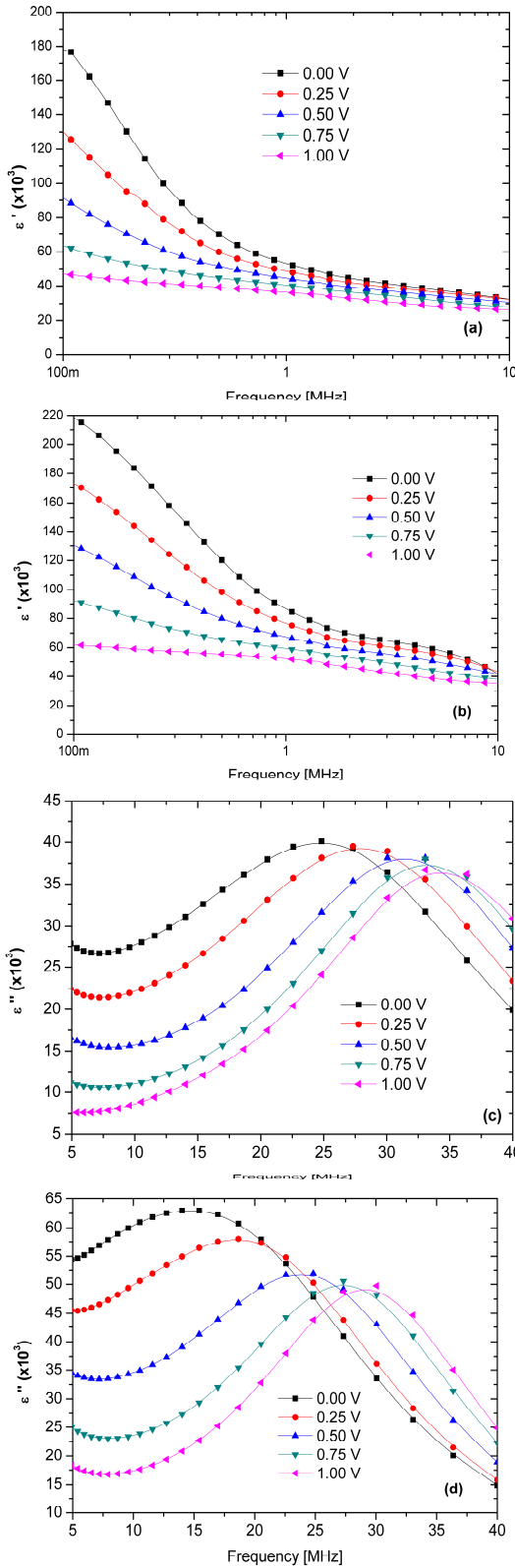


Figure 2. Frequency dependence of the dielectric constant at varying DC bias voltages; real part of: a) 15 Å, b) 20 Å, and imaginary part of: c) 15 Å, d) 20 Å thick Cr layer.

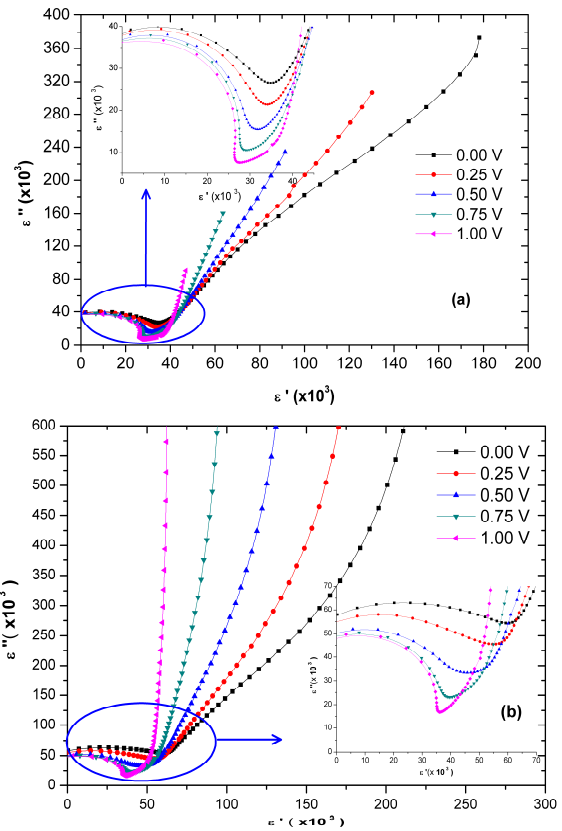


Figure 3. Cole-Cole plots of the samples at varying DC bias voltages; a) 15 Å b) 20 Å thick Cr layers.

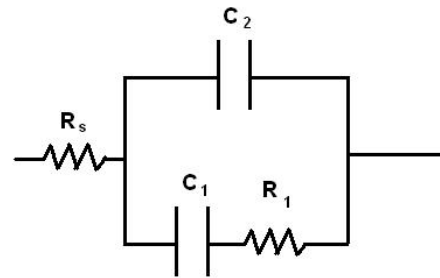


Figure 4. Equivalent circuit of the MTFs.

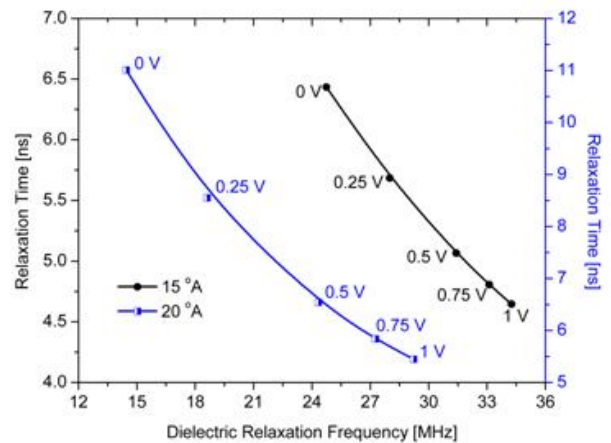


Figure 5. The relaxation time dependence on the dielectric relaxation frequency at varying DC bias voltages for two different multilayer ultrathin films.

Table 1. Dependence of f_c , α , and τ values on the thickness of Cr layer

MTF Samples (Bias Voltage= 0 V)	$f_c \times 10^7$ [Hz]	Adj. R-Square	α	$\tau \times 10^{-9}$ [s]
Cr 15 Å	2.53	0.99482	0.15525	6.73
Cr 20 Å	1.46	0.9795	0.10249	11.01

Table 2. $\Delta\epsilon$, f_c , τ , ϵ_{\max} values of MTFs under various DC bias voltages

Bias [Volts]	Cr 15 Å				Cr 20 Å			
	$\Delta\epsilon$	$f_c \times 10^7$ [Hz]	$\tau_{(\alpha=0)} \times 10^{-9}$ [s]	ϵ_{\max}	$\Delta\epsilon$	$f_c \times 10^7$ [Hz]	$\tau_{(\alpha=0)} \times 10^{-9}$ [s]	ϵ_{\max}
0.00	144971	2.47334	6.4348	40034	171791	1.44561	11.009	63027
0.25	97495	2.79932	5.6854	30335	129281	1.86118	8.5512	57979
0.50	60116	3.14149	5.0662	38111	88448	2.43352	6.5401	51417
0.75	35453	3.31070	4.8072	37587	54271	2.72592	5.8385	50407
1.00	20039	3.42517	4.6466	36713	26368	2.9225	5.4458	49650

Conclusions

Two MTFs, having different layer Cr thickness, were grown by magnetron sputtering deposition. These samples were characterized by impedance spectroscopy. A small change in the Cr layer thickness caused a substantial change in their dielectric properties. The relaxation process is found to be non-Debye type and became Debye type with the applied DC bias. An equivalent circuit diagram was constructed using the Cole-Cole plots. MTFs are promising elements in novel devices and their dielectric properties are of be useful in designing such devices.

REFERENCES

- Heinrich, B., J. F. Cochran, M. Kowalewski, J. Kirschner, Z. Celinski, A. S., Arrott, K. Myrtle, (1991) Magnetic anisotropies and exchange coupling in ultrathin fcc Co(001) structures, Phys. Rev. B, 44/17 9348–9361.
- Binasch, G., P. Grünberg, F. Saurenbach, W. Zinn, (1988) Enhanced magnetoresistance in layered magnetic structures with antiferromagnetic interlayer exchange, Phys. Rev. 39 7.
- Baibich, M.N., J.M. Broto, A. Fert, N. Van Dau, F. Petroof, P. Etienne, G. Creuzet, A. Friederich, J. Chazelas, (1988) Giant Magnetoresistance of (001)Fe/(001)Cr Magnetic Superlattices, Phys. Rev. Lett. 61 21.
- Galán, R.P., M.L. Calzada, L. Pardo, (2004) Reduced dielectric dispersion in ferroelectric (Pb, La)TiO₃/(Pb, Ca)TiO₃ thin-film multilayer heterostructures due to a mechanical stress relaxation mechanism, App. Phys. Lett. 84 4161.
- Kek-Merl, D., J. Lappalainen, H.L. Tuller, (2006) Electrical Properties of Nanocrystalline CeO₂ Thin Films Deposited by In Situ Pulsed Laser Deposition, J. Electrochem. Soc., 153/3 J15-J20.
- Wigen, P.E., Z. Zhang, (1992) Braz. J. of Phys., 22 4.
- du Tremolet de Lacheisserie, E., D. Gignoux, M. Schlenker, 2005 Magnetism–Materials & Applications, Kluwer Academic Publishers, Springer.
- Topkaya, R., M. Erkovan, A. Öztürk, O. Öztürk, B. Aktaş, and M. Özdemir, (2010) Ferromagnetic resonance studies of exchange coupled ultrathin Py/Cr/Py trilayers, Journal of Applied Physics, 108/2 023910.
- Knight, R.J., A. Nur, (1986) Dielectric enhancement due to the presence of thin gas pockets, Trans. Society of Professional Well Log Analysts Twenty Seventh Annual Logging Symposium, Paper JJ, 1 11.
- Raju, G.G. 2003 Dielectrics in Electric Fields (Marcel Dekker).
- Şentürk, E. (2004) Dielectric characteristics of a Ce³⁺-doped Sr_{0.61}Ba_{0.39}Nb₂O₆ single crystal with Cole-Cole plots technique, J. of Solid State Chemistry 177/4-5 1508-1512.
- Park, B.J., J.H. Sung, I.S. Lee, H.J. Choi, (2005) Comment on ‘Giant electrorheological activity of high surface area mesoporous cerium-doped TiO₂ templated by block copolymer’, Chem. Phys. Lett., 414/ 4-6 525.
- Macedo, P.B., C.T. Moynihan, R. Bose, (1972) Role of ionic diffusion in polarization in vitreous ionic conductors, Phys. Chem. Glasses, 13 171-179.
